12.

Tolerance modelling of stability of thin composite plates with dense system of beams

12.1. Introduction

The subject of the contribution are thin functionally graded skeletal plates with dense system of beams. The considered skeletal plate is made of two families of thin homogeneous beams with axes intersecting under the right angle. The regions situated between the beams fills a homogeneous matrix material (Fig. 12.1). It is assumed that the width of the beams can vary slowly in the midplane of the plate. Thus, we deal with composite plate that has space-varying microstructure. Since, the apparent properties of the plate are graded in space, we deal with a special case of a functionally graded material. The generalized period $l = \sqrt{l_1 l_2}$ of heterogeneity is assumed to be sufficiently small comparing to the measure of the midplane of the plate. The fundamental feature of proposed model is that the microstructure length parameter l is similar compared to thickness h of the plate. From a formal point of view, the plate with microstructure of this kind can be described in the framework of the well-known theories for thin elastic plates. However, due to the inhomogeneous microstructure of the plate, this direct description of the structure leads to plate equations with discontinuous and highly oscillating coefficients. These equations are not a good tool to be applied to numerical solutions of specific engineering problems.

The aim of the presented analysis is to derive and apply the macroscopic mathematical model describing stability of the composite plate under consideration. The macroscopic model for the plate dynamic analysis of this kind we can find in [12.5]. The formulation of the macroscopic mathematical model for the analysis of stability of these plates will to be based on the tolerance averaging approach. The general modelling procedures of this technique are given by Woźniak et al. in books [12.8], [12.9]. The applications of this technique for the modelling of stability of various periodic composites are given in a series of papers. Baron [12.1] analyzed dynamic stability of an uniperiodic medium thickness plate. In the paper of Michalak [12.3] the stability of elastic slightly wrinkled plates is analyzed. The stability of thin periodically stiffened cylindrical shells was analyzed by Tomczyk [12.6]. In the paper of Wierzbicki et al. [12.7], stability of micro-periodic materials under finite deformations is discussed. The approach, based on the tolerance averaging technique, formulating macroscopic model of stability of functionally graded plates was presented by Jędrysiak and Michalak [12.2]. In the paper of Perliński et al. [12.4] stability of functionally graded annular plate interacting with elastic micro-heterogeneous subsoil is presented.

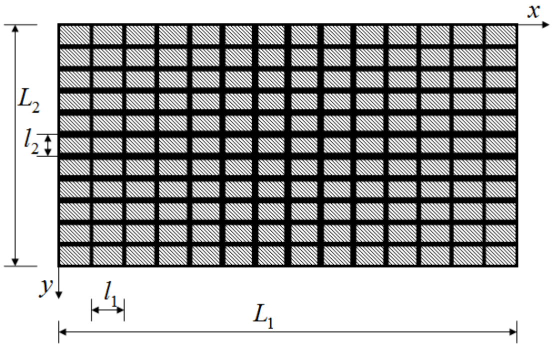

Fig. 12.1. Rectangular plate with varying width of the beams

In the above mentioned papers the thickness h of the considered plates is supposed to be much smaller comparing to the microstructure length parameter l. In the presented contribution we deal with the plates which are reinforced by two dimensional system of beams, where the microstructure length parameter $l = \sqrt{l_1 l_2}$ (l_1, l_2 - dimensions of cell in Fig. 12.1) is similar compared to the plate thickness h.

Throughout the contribution, indices $i, k, l \ldots$ run over $1,2,3$, indices $\alpha, \beta, \gamma, \ldots$ run over $1,2$ and $A, B, C, \ldots$ run over $1,2$. The summation convention holds all aforementioned sub-and superscripts.

12.2. Direct description

The subject of presented considerations are rectangular plates shown in Fig. 12.1. Let us introduce the orthogonal Cartesian coordinate system $Ox_1x_2x_3$. Setting $\mathbf{x} \equiv (x_1, x_2)$ and $z = x_3$ we assume that the undeformed plate occupies the region $\Omega \equiv \{(\mathbf{x}, z) : -h/2 \le z \le h/2, \mathbf{x} \in \Pi\}$, where Π is the plate midplane and h is the plate thickness. The starting point of this contribution is the direct description of the composite plate in the framework of the well-known second order non-linear theory of thin plates. The displacement field of the arbitrary point of the plate we write in form:

$$w_3(\boldsymbol{x},z)=w_3(\boldsymbol{x}), \qquad w_\alpha(\boldsymbol{x},z)=w_\alpha^0(\boldsymbol{x})-z\cdot\partial_\alpha w_3(\boldsymbol{x}) \tag{12.1}$$

Denoting by $\mathbf{p}(x_\alpha)$ the external forces, setting $\partial_k=\partial/\partial x_k$ we also introduce gradient operators $\nabla\equiv(\partial_1,\partial_2)$, in the framework of the linear approximated theory for thin plates, we obtain the following system of equations:

(i) strain-displacement relations

$$\begin{gathered} e_{\alpha\beta}(\boldsymbol{x},z)=\varepsilon_{\alpha\beta}(\boldsymbol{x})+\kappa_{\alpha\beta}(\boldsymbol{x})\cdot z \\ \varepsilon_{\alpha\beta}=\nabla_\beta w_\alpha^0+\tfrac{1}{2}\partial_\alpha w_3\ \partial_\beta w_3 \qquad \kappa_{\alpha\beta}=-\nabla_{\alpha\beta}w_3 \end{gathered} \tag{12.2}$$

(ii) strain energy averaged over the plate thickness

$$E(\boldsymbol{x})=\tfrac{1}{2}B^{\alpha\beta\gamma\delta}\,\kappa_{\alpha\beta}\,\kappa_{\gamma\delta}+\tfrac{1}{2}D^{\alpha\beta\gamma\delta}\varepsilon_{\alpha\beta}\ \varepsilon_{\gamma\delta} \tag{12.3}$$

where $D^{\alpha\beta\gamma\eta}=\dfrac{E\,h}{(1-\nu^2)}H^{\alpha\beta\gamma\eta}$ is the tensile stiffness and $B^{\alpha\beta\gamma\eta}=\dfrac{E\,h^3}{12(1-\nu^2)}H^{\alpha\beta\gamma\eta}$ with $H^{\alpha\beta\gamma\eta}=0.5(g^{\alpha\eta}\,g^{\beta\gamma}+g^{\alpha\gamma}g^{\beta\eta}+\nu(\in^{\alpha\gamma}\in^{\beta\eta}+\in^{\alpha\eta}\in^{\beta\gamma})$ is the bending stiffness.

(iii) work of external forces

$$F=p^\alpha\ w_\alpha^0+p^3\ w_3 \tag{12.4}$$

In order to derive governing equations of considered plate we shall define the stationary action functional:

$$\mathrm{A}(\mathbf{w}(\cdot))=\int_\Pi L(\mathbf{w},\nabla\mathbf{w},\nabla^2\mathbf{w})\,d\mathbf{x} \tag{12.5}$$

where Lagrangian $L=F-E$.

From stationary action principle ($\delta\mathrm{A}=0$) we obtain

$$\begin{gathered} \partial_{\alpha\beta}m^{\alpha\beta}-\partial_\alpha(n^{\alpha\beta}\,\partial_\beta w_3)=p^3 \\ \partial_\beta n^{\alpha\beta}=-p^\alpha \end{gathered} \tag{12.6}$$

where generalized forces

$$\begin{gathered} n^{\alpha\beta}=\int_{-h/2}^{h/2}\sigma^{\alpha\beta}dz=D^{\alpha\beta\gamma\delta}e_{\gamma\delta} \\ m^{\alpha\beta}=\int_{-h/2}^{h/2}\sigma^{\alpha\beta}z\,dz=B^{\alpha\beta\gamma\delta}\kappa_{\gamma\delta} \end{gathered} \tag{12.7}$$

This direct description leads to plate equations with discontinuous and highly oscillating coefficients, which are too complicated to be used in the engineering analysis. The above equations will be used as a starting point of the modelling procedure.

12.3. Modelling concept

Let the midplane of the considered plate (Fig. 12.1) occupy the region $\Pi \equiv [0, L_1] \times [0, L_2]$. We assume in considered composite plate that the number of beams in x_1 and x_2 direction is n and m, respectively $(1/n << 1, 1/m << 1)$. Hence $l_1 = L_1 / n$ and $l_2 = L_2 / m$ are dimensions of the cell $\Delta \equiv (-l_1/2, l_1/2) \times (-l_2/2, l_2/2)$, cf. Fig. 12.2. For the arbitrary cell $\Delta(\mathbf{x}) \equiv \Delta + \mathbf{x}$ with centre situated at point $\mathbf{x} = (x_1, x_2)$ we introduce the orthogonal local coordinate system Oy_1y_2 which is local with its origin at $\mathbf{x} \in \overline{\Pi}_\Delta$, where $\Pi_\Delta \equiv (l_1/2, L_1 - l_1/2) \times (l_2/2, L_2 - l_2/2) \subset \Pi$. The beams width is functional $a_\alpha = a_\alpha(\mathbf{x}), \alpha = 1,2$ but constant for every fixed $\mathbf{x} \in \overline{\Pi}_\Delta$.

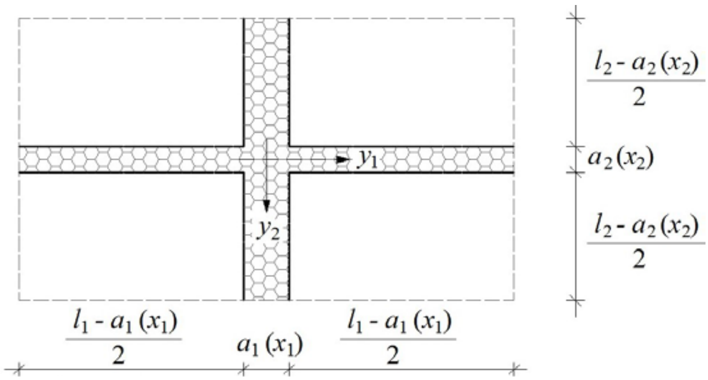

Fig. 12.2. A unit cell Δ geometry

In order to derive averaged equations for the plate under consideration we apply tolerance averaging approach [12.8, 12.9]. We mention here some basic concepts of this technique, as a tolerance periodic function, a slowly varying function, a highly oscillating function and an averaging operator.

The first concept of the modelling technique is *the averaging operation*:

$$< f > (\mathbf{x}) = \frac{1}{|\Delta|} \int_{\Delta(\mathbf{x})} f(\mathbf{y}, \mathbf{x}) d\mathbf{y}, \quad \mathbf{x} \in \overline{\Pi} \tag{12.8}$$

We shall refer (12.8) to as averaging of arbitrary integrable function $f(\cdot)$ for every $\mathbf{x} \in \overline{\Pi}$.

Periodic approximation. Let H^r be the Sobolev space for fixed $r \geq 0$. Function $\widetilde{f}^{(k)}(\mathbf{x},\cdot) \in H^0(\Pi)$, $\mathbf{x} \in \Pi$, $k = 1,2,...,r$ will be referred to as the periodic approximation of $\partial^k f(\cdot)$ in $\Delta(\mathbf{x})$ (where ∂^k - k-th gradient in Π). For $k = 0$ we define $\partial^0 f \equiv f$, $\widetilde{f}^{(0)} \equiv \widetilde{f}$.

Tolerance periodic function. Function $f \in H^r(\Pi)$ will be called *the tolerance periodic function* (with respect to cell $\Delta(\mathbf{x})$ and tolerance parameter ε), $f \in TP^r_\varepsilon(\Pi,\Delta)$, if for $k = 0,1,...,r,$ the following conditions hold:

$$\begin{aligned}
&(\forall \boldsymbol{x} \in \Pi)\left(\exists \widetilde{f}^{(k)}(\boldsymbol{x},\cdot) \in H^0(\Delta)\right)\left[\left\| \partial^k f(\cdot)\big|_{\Pi_x} - \widetilde{f}^{(k)}(\boldsymbol{x},\cdot)\right\|_{H^0(\Pi_x)} \leq \varepsilon\right] \\
&\int_{\Delta(\cdot)} \widetilde{f}^{(k)}(\cdot,\boldsymbol{y})\, d\boldsymbol{y} \in C^0(\overline{\Pi})
\end{aligned} \tag{12.9}$$

In the above definition we introduced the so called *cluster of cells*:

$$\Pi_x := \bigcap_{\mathbf{z}\in\Delta(\mathbf{x})} \Delta(\mathbf{z}), \quad \mathbf{x} \in \Pi_\Delta \tag{12.10}$$

Slowly varying function. Function $F \in H^r(\Pi)$ will be called *the slowly varying function* (with respect to the cell $\Delta(\mathbf{x})$ and tolerance parameter ε), and denoted by $F \in SV^r_\varepsilon(\Pi,\Delta)$, if for $k = 0,1,...,r,$ the following conditions hold:

$$F \in TP^r_\varepsilon(\Pi,\Delta) \text{ and } (\forall \mathbf{x} \in \Pi)\,[\widetilde{F}^{(k)}(\mathbf{x},\cdot)\,|_{\Delta(\mathbf{x})} = \partial^k F(\mathbf{x})] \tag{12.11}$$

It can be observed that periodic approximation $\widetilde{F}^{(k)}(\mathbf{x},\cdot)$ of $\partial^k F(\mathbf{x})$ in $\Delta(\mathbf{x})$ is a constant function for every $\mathbf{x} \in \Pi$. In other words, if $F \in SV^r_\varepsilon(\Pi,\Delta)$ then:

$$(\forall \mathbf{x} \in \Pi)\left(\left\|\partial^k F(\cdot) - \partial^k F(\mathbf{x})\right\|_{H^0(\Delta(\mathbf{x}))} \leq \varepsilon,\ k = 0,1,...,r\right) \tag{12.12}$$

Highly oscillating function. Function $\phi \in H^r(\Pi)$ is called *the highly oscillating function* (with respect to the cell $\Delta(\mathbf{x})$ and tolerance parameter ε), and denoted by $\phi \in HO^r_\varepsilon(\Pi,\Delta)$, if for $k = 0,1,...,r,$ the following conditions hold:

$$\begin{gathered}
\phi \in TP^r_\varepsilon(\Pi,\Delta) \\
(\forall \boldsymbol{x} \in \Pi)\,[\widetilde{\phi}^{(k)}(\boldsymbol{x},\cdot)\,|_{\Delta(x)} = \partial^k \widetilde{\phi}(\boldsymbol{x},\cdot)] \\
\forall F \in SV^r_\varepsilon(\Pi,\Delta)(f \equiv \phi F \in TP^r_\varepsilon(\Pi,\Delta)) \wedge \widetilde{f}^{(k)}(\mathbf{x},\cdot)\,|_{\Delta(\mathbf{x})} = F(\mathbf{x})\,\partial^k \widetilde{\phi}(\mathbf{x})\,|_{\Delta(\mathbf{x})}
\end{gathered} \tag{12.13}$$

Let by $\varphi(\cdot)$ denote a highly oscillating function, $\varphi \in HO^2_\varepsilon(\Pi,\Delta)$, defined on $\overline{\Pi}$, continuous together with gradient $\partial^1\varphi$. Its second derivative $\partial^2\varphi$ is a piecewise continuous and bounded. Function $\varphi(\cdot)$ is called *the fluctuation shape function* of the 2-nd kind, if it depends on l as a parameter and satisfies conditions:

1° $\partial^k \varphi \in O(l^{\alpha-k})$ for $k = 1,...,\alpha,\ \alpha = 2$,

2° $<\varphi>(\mathbf{x}) \approx 0$ for every $\mathbf{x} \in \Pi_\Delta$.

Set of all fluctuation shape functions of the 2-nd kind is denoted by $FS_\varepsilon^2(\Pi, \Delta)$.

12.4. Averaged model equations

The modelling technique will be based on the tolerance averaging approximation and on the restriction of the displacement field under consideration given by:

$$
\begin{aligned}
&w_3(\boldsymbol{x}, z) = V_3(\boldsymbol{x}) \\
&w_\alpha(\boldsymbol{x}, z) = V_\alpha(\boldsymbol{x}) + g^A(\boldsymbol{y}, \boldsymbol{x})V_\alpha^A(\boldsymbol{x}) + (-\partial_\alpha V_3(\boldsymbol{x}) + g^A(\boldsymbol{y}, \boldsymbol{x})u_\alpha^A(\boldsymbol{x}))\cdot z
\end{aligned}
\tag{12.14}
$$

for $\mathbf{x} \in \Pi$, $z \in (-h/2, h/2)$ and $A = 1,2$.

The basic tolerance modelling assumption states that macro-displacements $V_3(\cdot), V_\alpha(\cdot)$ and fluctuation amplitudes of displacements $V_\alpha^A(\cdot)$, $u_\alpha^A(\cdot)$ are slowly varying functions together with all partial derivatives. Functions $V_3(\cdot) \in SV_\varepsilon^2(\Pi, \Delta)$, $V_\alpha(\cdot) \in SV_\varepsilon^1(\Pi, \Delta)$, $u_\alpha^A(\cdot) \in SV_\varepsilon^1(\Pi, \Delta)$, $V_\alpha^A(\cdot) \in SV_\varepsilon^1(\Pi, \Delta)$ are the basic unknowns of the modelling problem. Functions $g^A(\cdot)$ are known, dependent on the microstructure length parameter $l = \sqrt{l_1 l_2}$ (l_1, l_2 - dimensions of the cell Δ), fluctuation shape functions.

Let $\tilde{g}^A(\mathbf{x},\cdot)$, $\partial_\alpha \tilde{g}^A(\mathbf{x},\cdot)$ stand for periodic approximation of $g^A(\cdot)$, $\partial_\alpha g^A(\cdot)$ in cell $\Delta(\mathbf{x})$, respectively. Due to the fact that $w_3(\cdot)$, $w_\alpha(\cdot)$ are tolerance periodic functions, it can be observed that the periodic approximation of $w_{3g}(\cdot, \mathbf{x})$, $w_{\alpha g}(\cdot, \mathbf{x})$ and their derivatives in $\Delta(\mathbf{x})$, $\mathbf{x} \in \Pi$ have the form:

$$
\begin{aligned}
&w_{3g}(\boldsymbol{y}, \boldsymbol{x}) = V_3(\boldsymbol{x}) \\
&\partial_\alpha w_{3g}(\boldsymbol{y}, \boldsymbol{x}) = \partial_\alpha V_3(\boldsymbol{x}) \\
&w_{\alpha g}(\boldsymbol{y}, \boldsymbol{x}, z) = V_\alpha(\boldsymbol{x}) + g^A(\boldsymbol{y}, \boldsymbol{x})V_\alpha^A(\boldsymbol{x}) + \left(g^A(\boldsymbol{y}, \boldsymbol{x})u_\alpha^A(\boldsymbol{x}) - \partial_\alpha V_3(\boldsymbol{x})\right)z \\
&\partial_\gamma w_{\alpha g}(\boldsymbol{y}, \boldsymbol{x}, z) = \partial_\gamma V_\alpha(\boldsymbol{x}) + \partial_\gamma g^A(\boldsymbol{y}, \boldsymbol{x})V_\alpha^A(\boldsymbol{x}) + \left(\partial_\gamma g^A(\boldsymbol{y}, \boldsymbol{x})u_\alpha^A(\boldsymbol{x}) - \partial_{\alpha\gamma} V_3(\boldsymbol{x})\right)z
\end{aligned}
\tag{12.15}
$$

Setting $w_3 = w_{3g}$ and $w_\alpha = w_{\alpha g}$ into Lagrangian $L(\mathbf{w}, \nabla\mathbf{w}, \nabla^2\mathbf{w})$ we can assume that $L_g(\mathbf{w}_g, \nabla\mathbf{w}_g, \nabla^2\mathbf{w}_g) \in HO_\varepsilon^0(\Pi, \Delta)$. Hence the periodic approximation of

$L_g(\cdot)$ in every $\Delta(\mathbf{x})$ we denote by $\widetilde{L}_g(\mathbf{x},\mathbf{y},w_{3g},w_{\alpha g},\partial_\alpha w_{3g},\partial_\alpha w_{\beta g})$. In order to derive the governing equations we shall define tolerance averaged Lagrangian $<L_g>=<F_g>-<E_g>$:

$$\begin{aligned}&<L_g>(\mathbf{x},\nabla_{\alpha\beta}V_3,\nabla_\alpha V_\beta,\nabla_\alpha V_3,V_3,V_\alpha,V_\alpha^A,u_\alpha^A)=\\&=\frac{1}{|\Delta|}\int\limits_{\Delta(\mathbf{x})}\widetilde{L}_g(\mathbf{x},\mathbf{y},w_{3g},w_{\alpha g},\partial_\alpha w_{3g},\partial_\alpha w_{\beta g})\,d\mathbf{y}\end{aligned}\tag{12.16}$$

Substituting the right-hand sides of equations (12.15) into (12.8), on the basis of tolerance averaging approximation, we arrive the strain energy averaged over the cell $\Delta(\mathbf{x})$:

$$\begin{aligned}&<E_g>=\tfrac{1}{2}<B^{\alpha\beta\gamma\delta}>\nabla_{\alpha\beta}V_3\nabla_{\gamma\delta}V_3-<B^{\alpha\beta\gamma\delta}\,\partial_\gamma g^A>u_\delta^A\nabla_{\alpha\beta}V_3+\\&+\tfrac{1}{2}<B^{\alpha\beta\gamma\delta}\partial_\beta g^A\partial_\delta g^B>u_\alpha^A u_\gamma^B+\tfrac{1}{2}<D^{\alpha\beta\gamma\delta}>\nabla_\beta V_\alpha\nabla_\delta V_\gamma+\\&+<D^{\alpha\beta\gamma\delta}\,\partial_\gamma g^A>V_\delta^A\nabla_\beta V_\alpha+\tfrac{1}{2}<D^{\alpha\beta\gamma\delta}\partial_\beta g^A\partial_\delta g^B>V_\alpha^A V_\gamma^B+\\&+\tfrac{1}{2}<D^{\alpha\beta\gamma\delta}>\nabla_\beta V_\alpha\nabla_\gamma V_3\nabla_\delta V_3+\tfrac{1}{2}<D^{\alpha\beta\gamma\delta}\partial_\beta g^A>V_\alpha^A\nabla_\gamma V_3\nabla_\delta V_3+\\&+\tfrac{1}{8}<D^{\alpha\beta\gamma\delta}>\nabla_\alpha V_3\nabla_\beta V_3\nabla_\gamma V_3\nabla_\delta V_3\end{aligned}\tag{12.17}$$

External load energy averaged over the cell $\Delta(\mathbf{x})$

$$<F_g>=<p^3>V_3+<p^\alpha>V_\alpha+<p^\alpha\,g^A>V_\alpha^A\tag{12.18}$$

From principle of stationary action of the averaged Lagrangian $<L_g>$ we obtain equations responsible for:

a) plane stress state

$$\begin{aligned}&\nabla_\beta N^{\alpha\beta}+<p^\alpha>=0\\&<n^{\alpha\beta}\,\nabla_\beta g^A>-<p^\alpha\,g^A>=0\end{aligned}\tag{12.19}$$

where normal forces

$$N^{\alpha\beta}=<n^{\alpha\beta}>=<D^{\alpha\beta\gamma\delta}>\nabla_\delta V_\gamma+<D^{\alpha\beta\gamma\delta}\,\nabla_\delta g^A>V_\gamma^A+\tfrac{1}{2}<D^{\alpha\beta\gamma\delta}>\nabla_\gamma V_3\,\nabla_\delta V_3\tag{12.20}$$

b) bending state

$$\begin{aligned}&\nabla_{\alpha\beta}\left(\widetilde{B}^{\alpha\beta\gamma\delta}\nabla_{\gamma\delta}V_3-\widetilde{B}^{\gamma A\alpha\beta}u_\gamma^A\right)-\nabla_\alpha\left(N^{\alpha\beta}\,\nabla_\beta V_3\right)-\left\langle p^3\right\rangle=0\\&\widetilde{B}^{\alpha A\gamma\delta}\nabla_{\gamma\delta}V_3-\widetilde{B}^{\alpha A\gamma B}u_\gamma^B=0\end{aligned}\tag{12.21}$$

where we have denoted:

$$\widetilde{B}^{\alpha\beta\gamma\delta} =< B^{\alpha\beta\gamma\delta} >, \widetilde{B}^{\alpha A\gamma\delta} =< B^{\alpha\beta\gamma\delta} \nabla_{\beta} g^{A} >, \widetilde{B}^{\alpha A\gamma B} =< B^{\alpha\beta\gamma\delta} \nabla_{\beta} g^{A} \nabla_{\delta} g^{B} > \tag{12.22}$$

From (12.21) we can obtain direct representation of oscillation amplitudes u_{γ}^{B}. Let $K_{\alpha\beta}^{AB}$ stands for linear transformation operator such that $K_{\alpha\tau}^{AC} \widetilde{B}^{\alpha A\gamma B} = \delta_{\tau\gamma}\delta^{BC}$. Thus

$$u_{\mu}^{B} = K_{\mu\alpha}^{BA} \widetilde{B}^{\alpha A\gamma\delta} \nabla_{\gamma\delta} V_{3} \tag{12.23}$$

Denoting

$$B_{eff}^{\alpha\beta\gamma\delta} = \widetilde{B}^{\alpha\beta\gamma\delta} - \widetilde{B}^{\mu B\alpha\beta} K^{\mu B\tau A} \widetilde{B}^{\tau A\gamma\delta} \tag{12.24}$$

stability equation takes a form

$$\nabla_{\alpha\beta}(B_{eff}^{\alpha\beta\gamma\delta} \nabla_{\gamma\delta} V_{3}) - \nabla_{\alpha}(N^{\alpha\beta} \nabla_{\beta} V_{3}) = 0 \tag{12.25}$$

The above equation has an identical form as stability equation for thin plate with functional coefficients. Coefficients in the above equation are functional but smooth in contrast to equation in direct description.

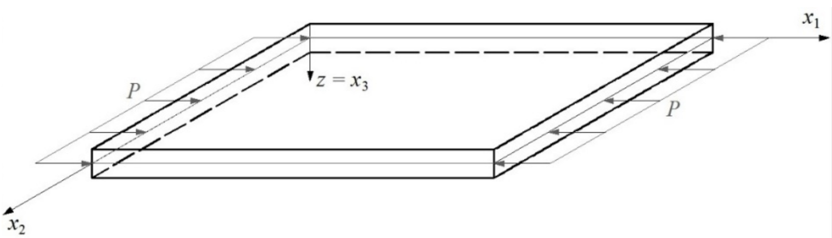

Fig. 12.3. Simply supported plate under pressure

12.5. Applications

Let us consider a rectangular plate simply supported on all edges and suppressed in one direction only, cf. Fig. 12.3. The stability equation (12.25) transforms then into:

$$\begin{aligned} &\partial_{11}\left(B_{eff}^{1111} \partial_{11} V_3 + B_{eff}^{1122} \partial_{22} V_3\right) + 4\partial_{12}\left(B_{eff}^{1212} \partial_{12} V_3\right) \\ &+ \partial_{22}\left(B_{eff}^{1122} \partial_{11} V_3 + B_{eff}^{2222} \partial_{22} V_3\right) - N^{11} \partial_{11} V_3 = 0 \end{aligned} \tag{12.26}$$

where $N^{11} = -P$. The above equation in all subsequent examples will be solved with Galerkin method using the following assumed form of solution:

$$V_3(\mathbf{x}) = \sum_{m=1}^{\infty}\sum_{n=1}^{\infty} V_{mn} \cdot \sin(\alpha_m x_1) \cdot \sin(\beta_n x_2) \tag{12.27}$$

where $\alpha_m = m\pi / L_1$, $\beta_n = n\pi / L_2$.

Since coefficients in (12.26) explicitly depend on assumed fluctuation shape functions, we must first define them, what is done next.

12.5.1. Fluctuation shape function

During tolerance modelling few assumptions had to be state. One of them is the form of given fluctuation shape functions. They should satisfy conditions mentioned in former sections and they are in number of two. Both of them are assumed as a product of linear and quadratic function

$$g^A(\mathbf{y},\mathbf{x}) = \varphi_1^{(A)}(\mathbf{y},\mathbf{x}) \cdot \varphi_2^{(A)}(\mathbf{y},\mathbf{x}) \tag{12.28}$$

where $A = 1,2$. Graphs of these functions are shown below (Fig.12.4a,12.4b).

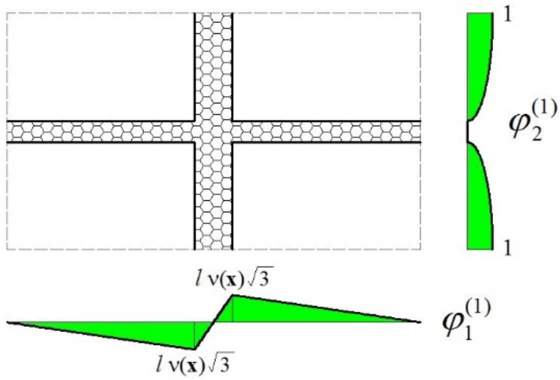

Fig. 12.4a. Fluctuation shape function g^1

Fluctuation shape functions depend on microstructure parameter l as well as on the distribution of heterogeneity:

$$v(\mathbf{x}) = \frac{1}{l^2}\sqrt{(l_1 - a_1(\mathbf{x}))(l_2 - a_2(\mathbf{x}))(l_1 a_2(\mathbf{x}) + l_2 a_1(\mathbf{x}) - a_1(\mathbf{x}) a_2(\mathbf{x}))} \tag{12.29}$$

Such properties and characteristics assure continuity of displacement field overall and stress field continuity along the beams.

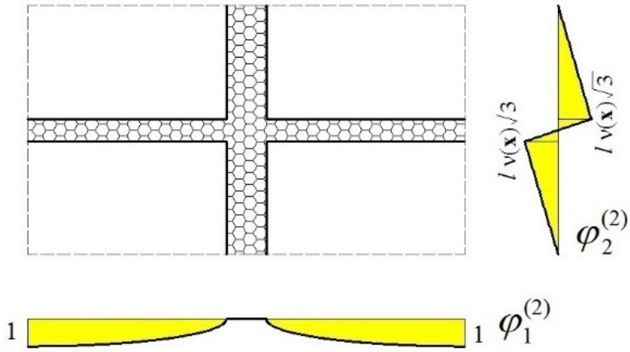

Fig. 12.4b. Fluctuation shape function g^2

The exact formulas of these functions:

$$\varphi_1^{(1)}(y_1,\mathbf{x}) = \begin{cases} \dfrac{2lv\sqrt{3}}{l_1-a_1}\left(y_1+\dfrac{l_1}{2}\right) & \text{for } y_1 \in \left[-\dfrac{l_1}{2},-\dfrac{a_1}{2}\right] \\ -\dfrac{2lv\sqrt{3}}{a_1} & \text{for } y_1 \in \left[-\dfrac{a_1}{2},\dfrac{a_1}{2}\right] \\ \dfrac{2lv\sqrt{3}}{l_1-a_1}\left(y_1-\dfrac{l_1}{2}\right) & \text{for } y_1 \in \left[\dfrac{a_1}{2},\dfrac{l_1}{2}\right] \end{cases} \tag{12.30}$$

$$\varphi_2^{(2)}(y_2,\mathbf{x}) = \begin{cases} \dfrac{2lv\sqrt{3}}{l_2-a_2}\left(y_2+\dfrac{l_2}{2}\right) & \text{for } y_2 \in \left[-\dfrac{l_2}{2},-\dfrac{a_2}{2}\right] \\ -\dfrac{2lv\sqrt{3}}{a_2} & \text{for } y_2 \in \left[-\dfrac{a_2}{2},\dfrac{a_2}{2}\right] \\ \dfrac{2lv\sqrt{3}}{l_2-a_2}\left(y_2-\dfrac{l_2}{2}\right) & \text{for } y_2 \in \left[\dfrac{a_2}{2},\dfrac{l_2}{2}\right] \end{cases} \tag{12.31}$$

$$\varphi_2^{(1)}(y_2,\mathbf{x}) = \begin{cases} 1-\left(\dfrac{l_2+2y_2}{l_2-a_2}\right)^2 & \text{for } y_2 \in \left[-\dfrac{l_2}{2},-\dfrac{a_2}{2}\right] \\ 0 & \text{for } y_2 \in \left[-\dfrac{a_2}{2},\dfrac{a_2}{2}\right] \\ 1-\left(\dfrac{l_2-2y_2}{l_2-a_2}\right)^2 & \text{for } y_2 \in \left[\dfrac{a_2}{2},\dfrac{l_2}{2}\right] \end{cases} \tag{12.32}$$

$$\varphi_1^{(2)}(y_1,\mathbf{x}) = \begin{cases} 1-\left(\dfrac{l_1+2y_1}{l_1-a_1}\right)^2 & \text{for } y_1 \in \left[-\dfrac{l_1}{2},-\dfrac{a_1}{2}\right] \\ 0 & \text{for } y_1 \in \left[-\dfrac{a_1}{2},\dfrac{a_1}{2}\right] \\ 1-\left(\dfrac{l_1-2y_1}{l_1-a_1}\right)^2 & \text{for } y_1 \in \left[\dfrac{a_1}{2},\dfrac{l_1}{2}\right] \end{cases} \tag{12.33}$$

12.5.2. Validation of proposed model

In order to find out the correctness of the proposed mathematical model and its applicability, some benchmark analysis should be first made. Suppose the beams (Fig. 12.2) are made of steel, i.e. for Young's modulus $E'' = 210\, GPa$ and Poisson's ratio $\nu'' = 0.3$, meanwhile the matrix is made of concrete for which has $E' = 20\, GPa$ and $\nu' = 0.3$. Consider a biperiodic square plate with $L_1 = L_2 = 4\, m$ and $l_1 = l_2$ of thickness $h = 0.1\, m$, which consists of beams (20 in each direction) of the same thickness: $a_1 = a_2$. Due to such a microstructure, all averaged coefficients in stability equation are constant and (12.26) reduces to:

$$B_{eff}^{1111}\partial_{1111}V_3 + 2\left(B_{eff}^{1122} + 2B_{eff}^{1212}\right)\partial_{1122}V_3 + B_{eff}^{2222}\partial_{2222}V_3 + P\,\partial_{11}V_3 = 0 \tag{12.34}$$

Now, substituting (12.27) we obtain:

$$P = \frac{\pi^2 B_{eff}^{1111}}{L_1^2}\cdot\frac{\sum_{m=1}^{\infty}\sum_{n=1}^{\infty}\left(m^4 + \eta\cdot m^2 n^2 + n^4\right)\cdot V_{mn}}{\sum_{m=1}^{\infty}\sum_{n=1}^{\infty} m^2\cdot V_{mn}} \tag{12.35}$$

where

$$\eta = \frac{2\left(B_{eff}^{1122} + 2B_{eff}^{1212}\right)}{B_{eff}^{1111}} \tag{12.36}$$

Hence the critical force for the *m*-th and *n*-th buckling mode:

$$P_{cr} = \frac{\pi^2 B_{eff}^{1111}}{L_1^2}\cdot\frac{m^4 + \eta\cdot m^2 n^2 + n^4}{m^2} \tag{12.37}$$

If $m = n = 1$ then we deal with the first mode of buckling.

Let us introduce a parameter $\beta = a_1 / l_1$, $\beta \in [0,1]$ as a volume fraction of beams material but in this example only. Case of $\beta = 0$ stands for an uniform plate made of matrix material (concrete) for which $P_{cr\_c} = 4.519 \cdot 10^3\ kN/m$, and case of $\beta = 1$ stands for uniform plate made of beams material (steel) for which $P_{cr\_s} = 4.745 \cdot 10^4\ kN/m$. These values for critical forces are obtained from the exact solution.

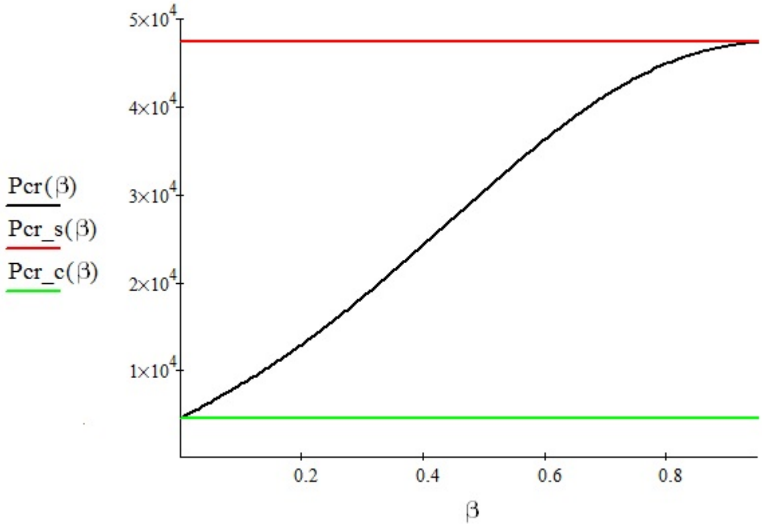

Fig. 12.5. Critical forces in square biperiodic plate as a function of parameter β

As we can see in Fig. 12.5, the graph is situated precisely between two values for uniform plate. Therefore, there exists a smooth passage from biperiodic to uniform plate which proofs the correctness of the proposed model.

12.5.3. Influence of geometrical and material properties on stability of plates

This section is devoted to some model applications presented in few numerical examples. Suppose the material properties of plate components are invariant in all following examples, i.e. we deal with concrete matrix and steel beams. Square plates ($L_1 = L_2 = 4\ m$) are only investigated.

Example 1. Suppose the width of the "vertical" beams $a_1 = l_1/4$, and width of the "horizontal" beams

$$a_2(\mathbf{x}) = a_2\left(\frac{l_2}{2}\right)\cdot\left[1+\left(\beta_2-1\right)\cdot\sin\left(\frac{\pi}{2}\cdot\frac{2x_2-l_2}{L_2-l_2}\right)\right] \tag{12.38}$$

for $x_2 \in \left[l_2/2, L_2 - l_2/2\right]$, where $a_2\left(l_2/2\right) = l_2/4$ and $\beta \equiv \beta_2 = a_2\left(L_2/2\right)/a_2\left(l_2/2\right)$ is a tested in this example parameter. Such width function implies uniperiodic plate with functionally graded effective properties in one of directions, cf. Fig. 12.6.

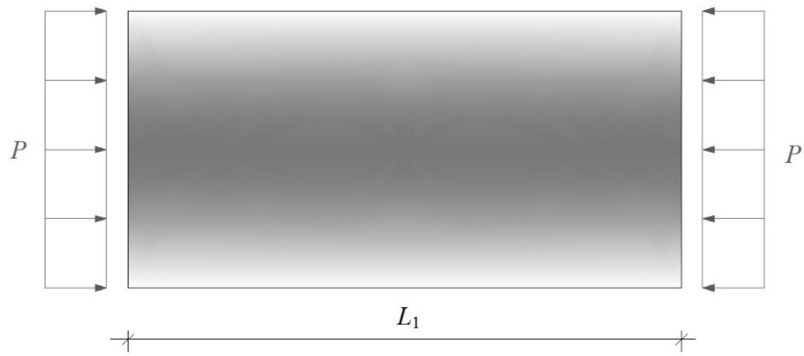

Fig. 12.6. Distribution of effective material properties in uniperiodic plate

Case of $\beta = 1$ stands here for biperiodic plate. If $\beta < 1$ then we deal with a situation where "horizontal" beams are getting wider moving away from the centre of the plate. Case of $1 < \beta \le 4$ is the opposite one.

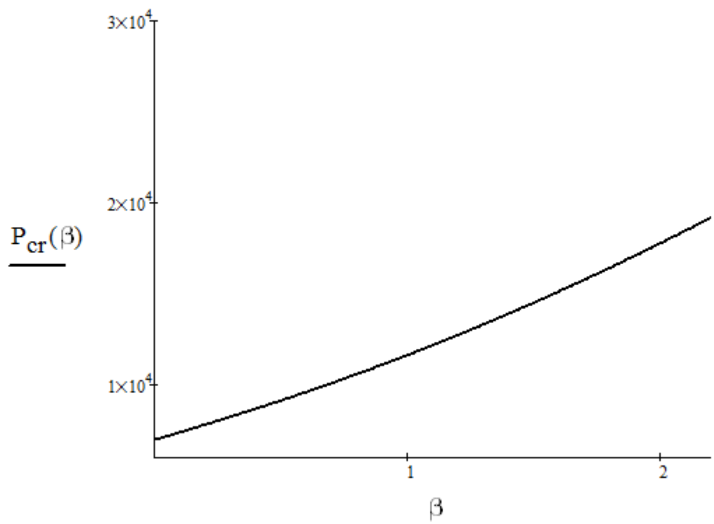

Fig. 12.7. Diagram of critical force in uniperiodic plate

The critical force as a function of parameter β is a strictly monotone (strictly increasing) function (Fig. 12.7). It means that concentration of beams material in the centre of the plate essentially enlarges the value of critical force.

Example 2. Suppose now that the width of vertical beams is not constant but expressed by similar form to (12.38):

$$a_1(\mathbf{x}) = a_1\left(\frac{l_1}{2}\right)\cdot\left[1+(\beta_1-1)\cdot\sin\left(\frac{\pi}{2}\cdot\frac{2x_1-l_1}{L_1-l_1}\right)\right] \tag{12.39}$$

for $x_1 \in [l_1/2, L_1 - l_1/2]$, where $a_1(l_1/2) = l_1/4$ and $\beta_1 = a_1(L_1/2)/a_1(l_1/2)$. The width of the "horizontal" beams is as in Example 1. Moreover, the same parameter β is investigated. Physical interpretation of β_1 is quite similar to β.

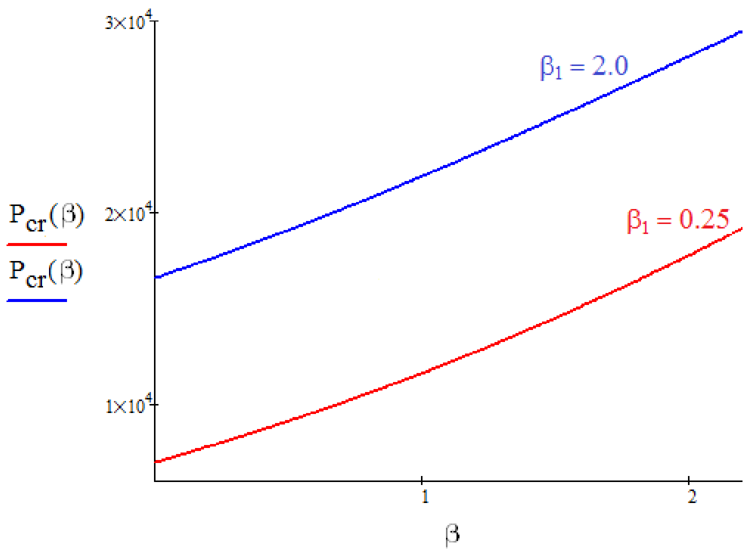

Fig. 12.8. Diagram of critical force in functionally graded plate

As we can see in Fig. 12.8, two graphs of critical force dependence for two different values of β_1 are displayed. Critical force is also strictly increasing with respect to parameter β_1. Thus, it suffices to have more beams material in the centre of the plate to obtain a greater value of critical force.

Example 3. The final example is most interesting in our opinion. Suppose

$$a_\alpha(\mathbf{x}) = \beta\cdot l_\alpha\cdot\sin\left(\frac{\pi}{2}\cdot\frac{2x_\alpha-l_\alpha}{L_\alpha-l_\alpha}\right) \tag{12.40}$$

for every $x_\alpha \in [l_\alpha / 2, L_\alpha - l_\alpha / 2]$, $\alpha = 1,2$, where $\beta \in [0,1]$. In Example 1 for $\beta_2 = 1$ we have dealt with biperiodic structure from which we can get the value of critical force $P_{cr\_per} = 1.552 \cdot 10^4 \ kN / m$ for some special case. In this particular case the volume fraction of the beam material was 0.25 (because of $\beta = 0.25$ from that example).

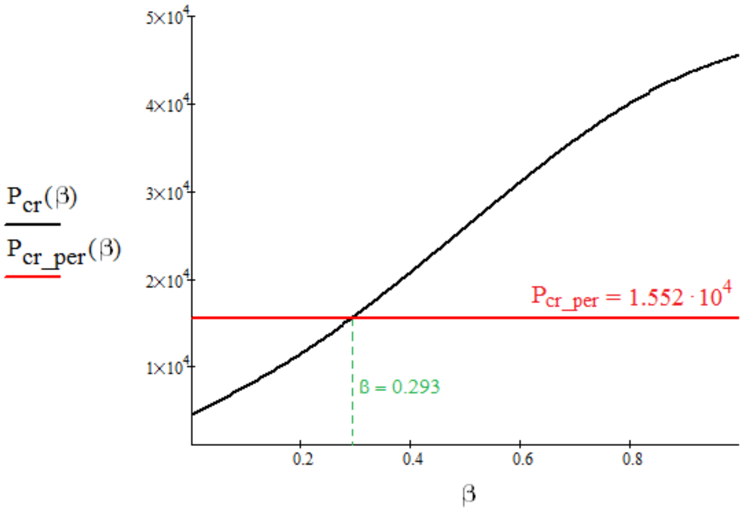

Fig. 12.9. Diagram of critical force in functionally graded plate in comparison to biperiodic plate

It occurs, Fig. 12.9, that the same value of critical force, but for the plate with variable beams width in both of directions, we obtained for $\beta = 0.293$. The beams material usage is 0.186 and its smaller then in biperiodic plate where it was 0.25. It means also that having variable beams width in our composite, by the same material usage in comparison to biperiodic structure, we get the greater values of critical force.

12.6. Summary

The problem of stability in two-component thin plates is described by the PDE with highly oscillating and discontinuous coefficients. Therefore, the tolerance technique was applied in order to obtain averaged PDEs with functional but smooth coefficients. Hence, the solution of specific boundary problems of stability of considered plates can be obtained using typical numerical method.

The validation process of the averaged model equations passed satisfactory. There is observed a smooth passage from non-uniform to uniform structure from the point of view of critical force value. It is obvious that reinforcement of the plate enlarge the value of this critical value but what is most important, the layout of these reinforcements (beams) plays crucial work in this analysis. It occurs that with non-uniform structure we can achieve up to 65% greater values of critical force the with biperiodic one. That information could be a crucial one in optimal control problems.

12.7. References

12.1 Baron E., On dynamic stability of an uniperiodic medium thickness plate band, J. Theor. Appl. Mech., Vol. 41, 2003, pp. 305-321.

12.2 Jędrysiak J., Michalak B., On the modelling of stability problems for thin plates with functionally graded structure. Thin-Walled Structures, Vol. 49, 2011, pp. 627-635.

12.3 Michalak B., Stability of elastic slightly wrinkled plates, Acta Mech., Vol. 130, 1998, pp. 111-119.

12.4 Perliński W., Gajdzicki M., Michalak B., Modelling of annular plates stability with functionally graded structure interacting with elastic heterogeneous subsoil, J. Theor. Appl. Mech., Vol. 52, 2014, pp. 485-498.

12.5 Rabenda M., Michalak B., Natural vibrations of prestressed thin functionally graded plates with dense system of ribs in two directions, Composite Structures, Vol. 133, 2015, pp. 1016-1023.

12.6 Tomczyk B., On stability of thin periodically densely stiffened cylindrical shells, J. Theor. Appl. Mech., Vol. 43, 2005, pp. 427-455.

12.7 Wierzbicki E., Woźniak Cz., Woźniak M., Stability of micro-periodic materials under finite deformations, Arch. Mech., Vol. 49, 1997, pp. 143-158.

12.8 Woźniak Cz., Michalak B.,Jędrysiak J., (eds.), Thermomechanics of Heterogeneous Solids and Structures, Wydawnictwo Politechniki Łódzkiej, Łódź 2008.

12.9 Woźniak Cz., et al., (eds.), Mathematical modeling and analysis in continuum mechanics of microstructured media, Wydawnictwo Politechniki Śląskiej, Gliwice 2010.